Theor Chem Acc (2012) 131:1119
DOI 10.1007/s00214-012-1119-9

REGULAR ARTICLE

# Theoretical study for the $CH_3OCF_2CF_2OCHO$ + Cl reaction

**Tong-yin Jin · Hong-bo Yu · Cheng-gang Ci · Jing-yao Liu**

Received: 2 May 2011 / Accepted: 14 August 2011 / Published online: 9 February 2012


**Abstract** The reaction of $CH_3OCF_2CF_2OCHO$ with Cl atom has been investigated theoretically by direct dynamics method. The BB1K hybrid functional in conjunction with the 6-31 + G(d,p) basis set has been used to optimize the geometries for the stationary points and explore the potential energy surface of the reaction. Four rotation conformers (RC1-4) of $CH_3OCF_2CF_2OCHO$ are identified, and they are all considered in the kinetic calculation. For each conformer, there are two kinds of H-abstraction channels and one displacement channel, and the latter one should be negligible due to involving much higher energy barrier than the former two. The individual rate constants for each H-abstraction channel are evaluated by the improved canonical variational transition-state theory with a small-curvature tunneling correction. The overall rate constant is evaluated by the Boltzmann distribution function, and a fitted four-parameter rate constant expression is obtained over a wide temperature range of 200–2,000 K. The agreement between the calculated and available experimental value at 296 K is good. The contribution of each conformer to the title reaction is discussed with respect to the temperature. In addition, because of the lack of available experimental data for the species involved in the reactions, the enthalpies of the formation ($\Delta H_{f,298^\circ}$) for the reactant and its product radicals are predicted via isodesmic reaction at the BB1K/6-31 + G(d,p) level.

**Keywords** Direct dynamics · Rate constant · Variational transition-state theory · Hydrogen abstraction · $CH_3OCF_2CF_2OCHO$

## 1 Introduction

Owing to the well-known adverse environmental impact of chlorofluorocarbons (CFCs), many efforts have been devoted to developing the environmentally acceptable alternatives such as hydrofluorocarbons (HFCs) and hydrofluoroethers (HFEs) to CFCs. Recently, a new class of hydrofluoropolyethers (HFPEs) with a structure of $CH_3O(CF_2CF_2O)_nCH_3$ was found to have low toxicity and some other remarkable properties of similar perfluorinated compounds [1–4] and thus has been suggested as potential CFC replacements. The atmospheric oxidation of HFPEs gives the fluoridated formate $CH_3O(CF_2CF_2O)_nCHO$. So, the problems arise: Do these formates pose any significant environmental hazard? What are the atmospheric fates of them? On the other hand, because of the higher reactivity toward most organic compounds and substantial concentration in the coastal areas and industrial zones, Cl atom may play an important role in the degradation of these compounds under atmospheric condition. In our previous study, we reported the rate constants of the $CH_3OCF_2CF_2OCH_3$ + Cl reaction over a wide temperature range of 200–2,000 K [5]. In order to assess the environmental impact and provide a more complete picture of the atmospheric degradation mechanism of $CH_3OCF_2CF_2OCF_3$, a better understanding of the atmospheric removal mechanism of its oxidation product $CH_3OCF_2CF_2OCHO$ is very necessary. Experimentally, only one kinetic study of the $CH_3OCF_2CF_2OCHO$ + Cl reaction was performed by Wallington et al. [6], and the overall rate constant was

**Electronic supplementary material** The online version of this article (doi:10.1007/s00214-012-1119-9) contains supplementary material, which is available to authorized users.

T. Jin · H. Yu · C. Ci · J. Liu (✉)
State Key Laboratory of Theoretical and Computational Chemistry, Institute of Theoretical Chemistry, Jilin University, Changchun 130023, People's Republic of China
e-mail: ljy121@jlu.edu.cn

determined to be $(1.81 \pm 0.36) \times 10^{-13}$ $cm^3$ $molecule^{-1}$ $s^{-1}$ at 296 ± 3 K by using relative rate techniques.

For the reaction $CH_3OCF_2CF_2OCHO + Cl$, it is easily found that more than one channel are available at different sites of $CH_3OCF_2CF_2OCHO$. For example, the reaction may take place via the H-abstraction channels from the $–CH_3$ and –CHO groups, leading to different product isomers or via the displacement channel. However, there is a lack of relevant theoretical reports on the reaction mechanism as well as the rate constants at other temperatures to the best of our knowledge. Therefore, in the present work, we employed density function theory (DFT) direct dynamics method to study the reaction. The potential energy surface (PES) information was obtained by BB1K method [7], then the rate constants and the branching ratios of different channels were calculated using the variational transition-state theory (VTST) [8–10] over a temperature range of 200–2,000 K. The comparison and discussion between theory and experiment were made. Our aim is to gain a deeper insight into the mechanism and kinetics of the reaction and fill a void in the available data for atmospheric chemistry.

## 2 Calculation method

In the present work, all the electronic structure calculations were performed with the GAUSSIAN 09 program [11]. The optimized geometries of the stationary points were calculated at a hybrid Hartree-Fork-density functional model BB1K (Becke88 [12]-Becke95 [13] one-parameter model for kinetics) in combination with the 6-31 + g(d,p) basis set (BB1K/6-31 + g(d,p)). The reliability and efficiency of the BB1K/6-31 + g(d,p) level of theory have been verified by Truhlar et al. [14] and successfully applied in many radical reactions [15–17]. Each stationary point was characterized by the harmonic vibrational frequency analysis. The number of imaginary frequencies (0 or 1) indicates whether a minimum or a transition state has been located. At the same level, the minimum-energy path (MEP) is calculated with intrinsic reaction coordinate (IRC) theory to confirm that the transition state (TS) really connects the reactant and product. Also, the energy derivatives including gradients and Hessians at geometries along the MEP were obtained to calculate the curvature of the reaction path.

On the basis of the initial PES information, the kinetics calculations were performed with the POLYRATE 9.7 program [18]. The theoretical rate constants were calculated using the improved canonical variational transition-state theory (ICVT) [19] with the small-curvature tunneling (SCT) [20, 21] correction over the temperature range of 200–2,000 K. During the kinetic calculations, the Euler single-step integrator with a step size of 0.001 $(amu)^{1/2}$ is used to follow the MEP, and the generalized normal-mode analysis is performed every 0.01 $(amu)^{1/2}$ Bohr. Most of the vibrational modes were treated as quantum–mechanical separable harmonic oscillators, while the lower modes associated with torsion was treated as hindered rotor. The hindered-rotor approximation [22–24] was used for calculating the partition functions of the torsion modes. The vibrational frequencies corresponding to the hindered rotor are labeled in the tables (see Table 1 in the text and Table S1 in Supporting Information). The C$\omega$ scheme [25–27], which was the recommended method in Reference [28, 29], was applied for treating the hindered rotor. In this scheme, the moment of inertia for the minimum-energy point of the internal rotation potential curve is calculated by a curvilinear (C) model [23], harmonic-oscillator frequencies are obtained by electronic structure calculations, and the barrier of internal rotation is calculated by

$$W_j = 2I_j(\omega_j/M)^2$$

where $I_j$ is the moment of inertia for internal rotation, $\omega_j$ is the vibrational frequency, and M is the total number of minima along the torsional coordinate in the range 0–2$\pi$ [25]. For each torsion mode, the number of distinct minima along the torsional coordinate is 3, and the symmetry number of the minimum has a value of 1, that is, $M = 3$. In the calculation of the electronic partition functions, the $^2P_{3/2}$ and $^2P_{1/2}$ electronic states of Cl atom were included, with an 881 $cm^{-1}$ splitting due to the spin-orbital coupling.

## 3 Results and discussion

### 3.1 Stationary points

With respect to the reactant $CH_3OCF_2CF_2OCHO$, we located four stable rotation conformers, denoted as RC1, RC2, RC3, and RC4, as well as four transition states for the interconversion of them. The potential energy profile connecting them is shown in Fig. 1, and some of the key optimized geometric parameters for RC1-4 are shown in Fig. 2. It is clearly seen from the schematic configurations of the four conformers in Fig. 1 that RC1 can be transformed into RC3 by a rotation of $–CF_2OCH_3$ group around the C–C axis, with a rotation barrier of 3.86 kcal/mol. By a –CHO group rotation of 180°, RC1 and RC3 can be transformed into RC2 and RC4, respectively. The rotation barriers are 6.96 kcal/mol between RC1 and RC2 and 6.50 kcal/mol between RC3 and RC4. Also, it is shown that RC1 and RC3 are the most stable conformers, while RC2 and RC4 are 0.41 and 0.83 kcal/mol higher in energy than them. Note that the energies of the two conformers RC1 and RC3 are not exactly same; if the

**Table 1** Calculated frequencies ($cm^{-1}$) of the four reactant conformers, and the products and TSs of the H-abstraction reactions of RC1 at the BB1K/6-31 + G(d,p) level

| Species | Frequencies |
|---|---|
| RC1 | 51,56[a],71,115,167,177,213,217,298,312,372,396,524,546,606,626,670,821,881,1052,1063,1146,1191,1209,1217,1234,1247,1282, 1333,1437,1489,1526,1538,1540,1941,3139,3187,3231,3267 |
| RC2 | 48[a],71,85,118,136,154,185,251,290,334,372,387,494,540,568,619,674,803,904,1041,1058,1111,1192,1199,1208,1231,1244,1291, 1334,1471,1497,1522,1530,1538,1962,3140,3161,3233,3270 |
| RC3 | 42,57[a],79,100,174,177,213,223,262,339,370,390,524,548,595,633,666,821,882,1038,1063,1163,1193,1196,1213,1238,1240,1281, 1336,1437,1484,1530,1535,1538,1941,3139,3187,3231,3269 |
| RC4 | 46[a],76,96,108,154,183,222,228,301,344,377,384,493,543,560,629,674,805,896,1038,1065,1127,1186,1200,1213,1239,1240,1293, 1338,1489,1504,1531,1535,1538,1963,3140,3162,3234,3270 |
| P1a-1 | 53,57,91,119,171,196,213,314,297,313,375,396,522,545,571,606,626,669,817,881,1062,1099,1185,1202,1225,1234,1254,1285, 1338,1436,1489,1512,1943,3191,3251,3410 |
| P1a-2 | 52,57,84,120,167,193,213,215,292,314,372,399,523,539,557,606,626,669,815,881,1062,1099,1186,1198,1223,1235,1253,1286, 1338,1436,1489,1505,1943,3190,3250,3410 |
| P1b | 47,53,67,115,166,173,208,261,291,312,372,396,525,544,605,622,662,819,872,1048,1135,1151,1198,1208,1215,1243,1293,1335, 1480,1524,1529,1538,1983,3141,3234,3270 |
| HCl | 3078 |
| TS1a-1 | 887i,21,43,51,66[a],110,135,166,206,214,281,313,371,390,413,514,528,544,608,626,670,817,878,1001,1029,1063,1099,1176,1213, 1232,1239,1251,1264,1289,1321,1436,1484,1513,1944,3188,3198,3323 |
| TS1a-2 | 903i,16,39,53,64[a],103,137,169,200,213,288,312370,385412,510,524,549,607,627,668,817,880,990,1022,1061,1099,1177,1208, 1233,1238,1254,1262,1293,1323,1435,1484,1519,1946,3188,3194,3322 |
| TS1b | 1020i,32,42,47,71[a],72,129,154,166,21,284,306,322,337,373,402,539,545,608,625,699,824,882,887,1011,1052,1144,1187,1203, 1212,1221,1245,1306,1340,1482,1525,1529,1536,1996,3142,3237,3274 |

[a] Torsion mode

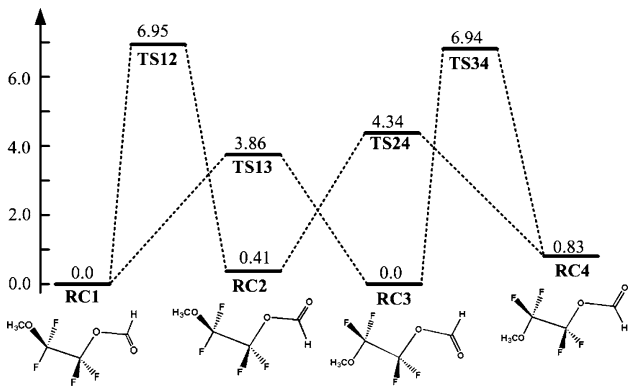


**Fig. 1** Schematic potential energy profile for the isomerization reactions among RC1, RC2, RC3, and RC4. Relative energies (in kcal/mol) are calculated at the BB1K/6-31 + G (d,p) + ZPE level

energy of RC1 is set to the zero as reference, the relative energy of RC3 is 0.06 kcal/mol without ZPE and −0.002 kcal/mol with ZPE. So when the results are given to a hundredth of a kcal, they are considered in the same energy. In addition, because of the small energy differences among them, all of the four conformers are considered in the present study.

For each conformer as shown in Fig. 2, the reaction may take place via the hydrogen abstraction by Cl atom from either $–CH_3$ or –CHO group. Since both RC1 and RC2 have $C_1$ symmetry and none of the three hydrogen atoms ($H_a$, $H_b$, and $H_c$) in the $–CH_3$ group is equivalent, three distinct H-abstraction channels should be available. However, for the RC1 + Cl (or RC2 + Cl) reaction, only two distinct channels are found for the abstraction from $H_b$ and $H_c$ atoms in the $–CH_3$ group, namely R1a-1 and R1a-2 for RC1 (or R2a-1 and R2a-2 for RC2), respectively. In our optimization calculations, it is found that when Cl atom approaches the $H_a$ hydrogen in RC1 (or RC2), the $–CH_3$ group and the Cl atom will rotate simultaneously around the C–O bond, leading to the same transition-state structure as TS1a-2 (or TS2a-2). The IRC calculations further confirm that transition states TS1a-2 and TS2a-2 connect to the initial configurations in which Cl atom approaches $H_c$ atom of RC1 and RC2, respectively, which means that the H-abstraction channel from $H_a$ is infeasible for RC1 and RC2. Moreover, one channel is found for the H-abstraction from the –CHO group for RC1 and RC2, denoted as R1b and R2b, respectively. Similarly, in the case of conformers RC3 and RC4 with $C_S$ symmetry, the optimization of the TS for the H-abstraction from the in-plane hydrogen ($H_a$) failed, so only one H-abstraction channel from the out-of-plane hydrogen ($H_b$) of the $–CH_3$ group and one H-abstraction from the –CHO group are located. For the displacement process, the attack of Cl at the α-C in the molecule is considered for each conformer.

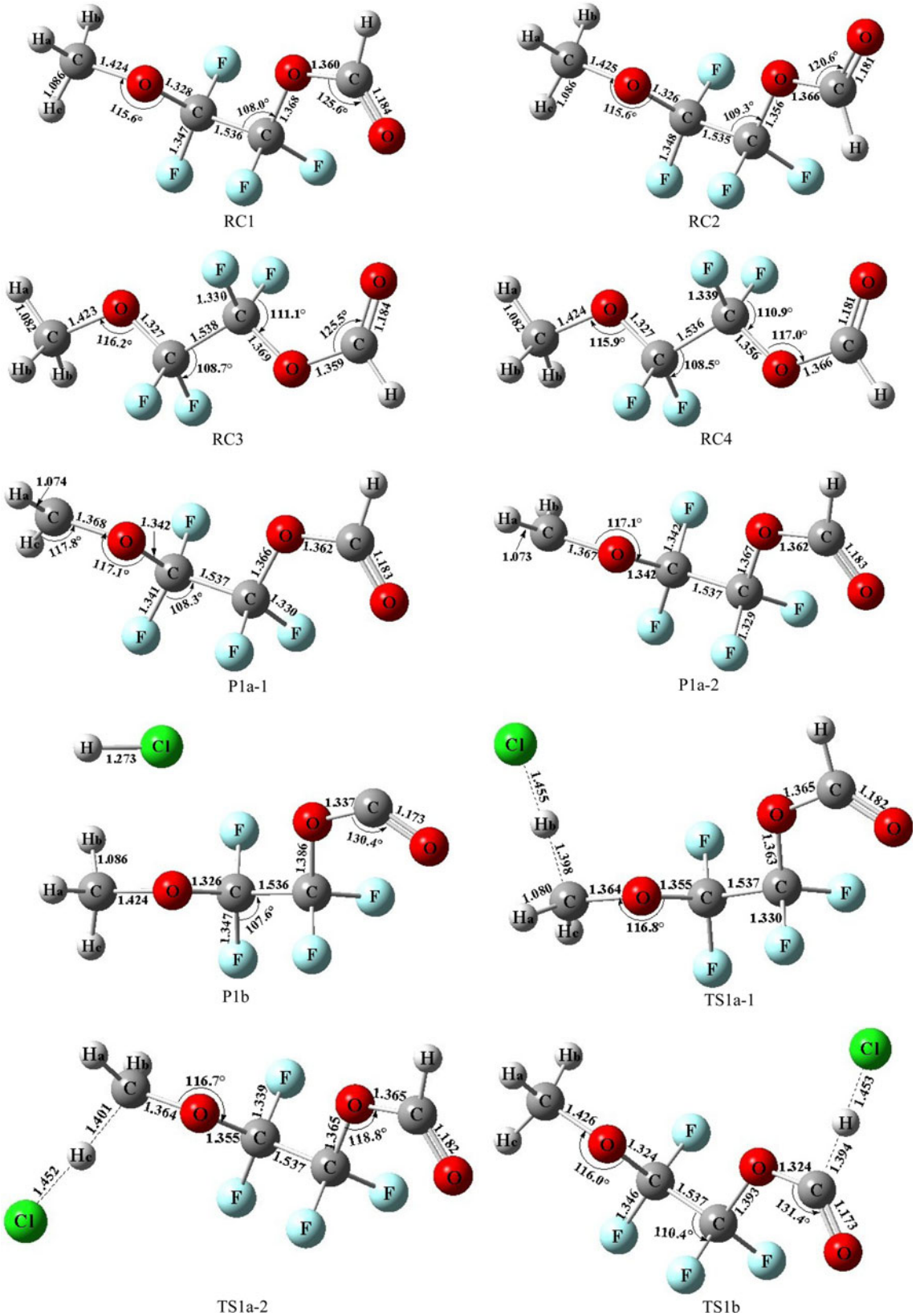


**Fig. 2** Optimized geometries parameters (in Å and degree) of the four reactant conformers, and the products and TSs of the H-abstraction reactions of RC1 at the BB1K/6-31 + G(d,p) level

$$CH_3OCF_2CF_2OCHO + Cl \rightarrow CH_2OCF_2CF_2OCHO + HCl \quad (Rna\text{-}1,\ Rna\text{-}2,\ n = 1, 2;\quad Rna,\ n = 3,\ 4)$$
$$\rightarrow CH_3OCF_2CF_2OCO + HCl \quad (Rnb,\ n = 1\text{-}4)$$
$$\rightarrow OCF_2CF_2OCHO + CH_3Cl \quad (Rnc,\ n = 1\text{-}4)$$

The key optimized geometric parameters and harmonic vibrational frequencies for the product radicals and transition states involved in the hydrogen abstraction channels of RC1 are shown in Fig. 2 and Table 1, respectively, and the geometric structures and frequencies of other stationary points in the four reactions (R1-4) are given in Supporting Information (see Fig. S1 and Table S1). The reactants and products have only real frequencies, while the transition states are confirmed to have only one imaginary frequency corresponding to the stretching mode of the coupling between the breaking and forming bonds. In the TS structures of the H-abstraction channels, the elongation of the breaking bond is greater than that of the forming bond, indicating that the TSs are more similar to the products than to the reactants. For example, the length of the breaking C–H bond in TS1a-1 is elongated by 28% compared to the equilibrium C–H bond length in the isolated reactants, and the forming H–Cl bond is stretched by 14% with respect to the equilibrium bond length of HCl. Similar cases can be found for other TSs.

Schematic potential energy surface of the $CH_3OCF_2CF_2OCHO + Cl$ reaction obtained at the BB1K/6-31 + G(d,p) level with the ZPE corrections is plotted in Fig. 3. The energy of the reactants is set to zero as a reference. As can be seen from Fig. 3a–d, for each conformer, the displacement channel is kinetically and thermodynamically infeasible due to the much higher energy barriers (about 35 kcal/mol higher than those of the H-abstraction channels) and endothermicity of about 10 kcal/mol, thus its contribution to the title reaction should be negligible. For the three H-abstraction channels of RC1, the relative energies of the transition states for the H-abstractions from the $–CH_3$ group (TS1a-1 and TS1a-2) are slightly lower than that for the H-abstraction from the –CHO group (TS1b) by 0.8 and 0.43 kcal/mol, respectively; as a result, just from energetic point of view, it is predicted that the reaction may take place mainly via the H-abstraction from the $–CH_3$ group, while the abstraction channel from –CHO group may be competitive. Similar conclusion can be drawn for the other conformers. Moreover, the reaction enthalpies ($\Delta H_{298^\circ}$) calculated at the BB1K/6-31G + (d,p) level for the H-abstraction channels are listed in Table 2. It is seen that the reaction channels R1a-1, R1a-2, R1b, R2a-1, R2a-2, R3a, R3b, and R4a are almost thermal neutral, while R2b and R4b are slightly exothermic, with the values of −3.98 and −4.06 kcal/mol, respectively.

A reliable enthalpy of formation ($\Delta H_{f,298^\circ}$) of the species plays an important role in the atmospheric modeling. Since there are no relevant experimental or theoretical estimations for the $\Delta H_{f,298^\circ}$ values of the reactant $CH_3OCF_2CF_2OCHO$ and its product radicals, we evaluated their $\Delta H_{f,298^\circ}$ values using the following group-balanced isodesmic reactions:

$$CH_3OCF_2CF_2OCHO + 2CH_3F \rightarrow CH_3OCH_3 + CF_3CF_3 + CH_3OCHO \quad (R5)$$
$$CH_2OCF_2CF_2OCHO + 2CH_3F + CH_3CH_3 \rightarrow CH_2CH_3 + CH_3OCH_3 + CF_3CF_3 + CH_3OCHO \quad (R6)$$
$$CH_3OCF_2CF_2OCO + 2CH_3F + CH_3CH_3 \rightarrow 2CH_3OCH_3 + CF_3CF_3 + CH_3CO \quad (R7)$$

Here, the geometries and frequencies of the stationary points involved in these reactions R5-7 are obtained at the same BB1K/6-31 + G(d,p) level of theory. Note that only the electronic structure information of conformer RC1 and the corresponding product radicals was used in the above calculations, and it is easy to obtain the $\Delta H_{f,298^\circ}$ values for the other conformers by adding the enthalpy differences between them. The calculated reaction enthalpies of R5-7 are combined with the known standard enthalpies of formation [30] ($CH_3F$: −56.0 kcal/mol; $CH_3OCH_3$: −44.0 ± 0.12 kcal/mol; $CF_3CF_3$: −321.19 kcal/mol; $CH_3OCHO$: −80.52 kcal/mol; $CH_3CH_3$: −20.04 ± 0.07 kcal/mol; $CH_2CH_3$: 28.44 ± 0.49 kcal/mol; and $CH_3CO$: −2.87 ± 0.71 kcal/mol) to evaluate the enthalpies of formation of these species. The calculated results (listed in Table 3) are −328.14 ± 0.1 kcal/mol for RC1, −279.95 ± 0.6 kcal/mol for P1a-1, and −286.07 ± 0.71 kcal/mol for P1b.

### 3.2 Rate constant calculations

The individual improved canonical variational transition-state theory with a small-curvature tunneling correction (ICVT/SCT) rate constants of each H-abstraction channel of the four conformers is calculated over a wide temperature region from 200 to 2,000 K. The total rate constants of each reaction (R1-4) are obtained from the sum of the individual rate constants, that is, $k_n = k_{na-1} + k_{na-2} + k_{1b}$ ($n = 1, 3$), $k_n = k_{na} + k_{nb}$ ($n = 2, 4$), and the results are listed in Table 4. The temperature dependence of the branching ratios for each reaction is plotted in Fig. 4. It is seen that, for the RC1 + Cl reaction, the branching ratios of $k_{1a\text{-}1}/k_1$, $k_{1a\text{-}2}/k_1$, and $k_{1b}/k_1$ are 0.61, 0.27, and 0.12 at 200 K, 0.36, 0.31, and 0.33 at 500 K, and 0.24, 0.28, and 0.48 at 2,000 K, respectively, which means that R1a-1 is the dominant reaction channel of R1 at the low temperature, while R1b is more and more important as temperature

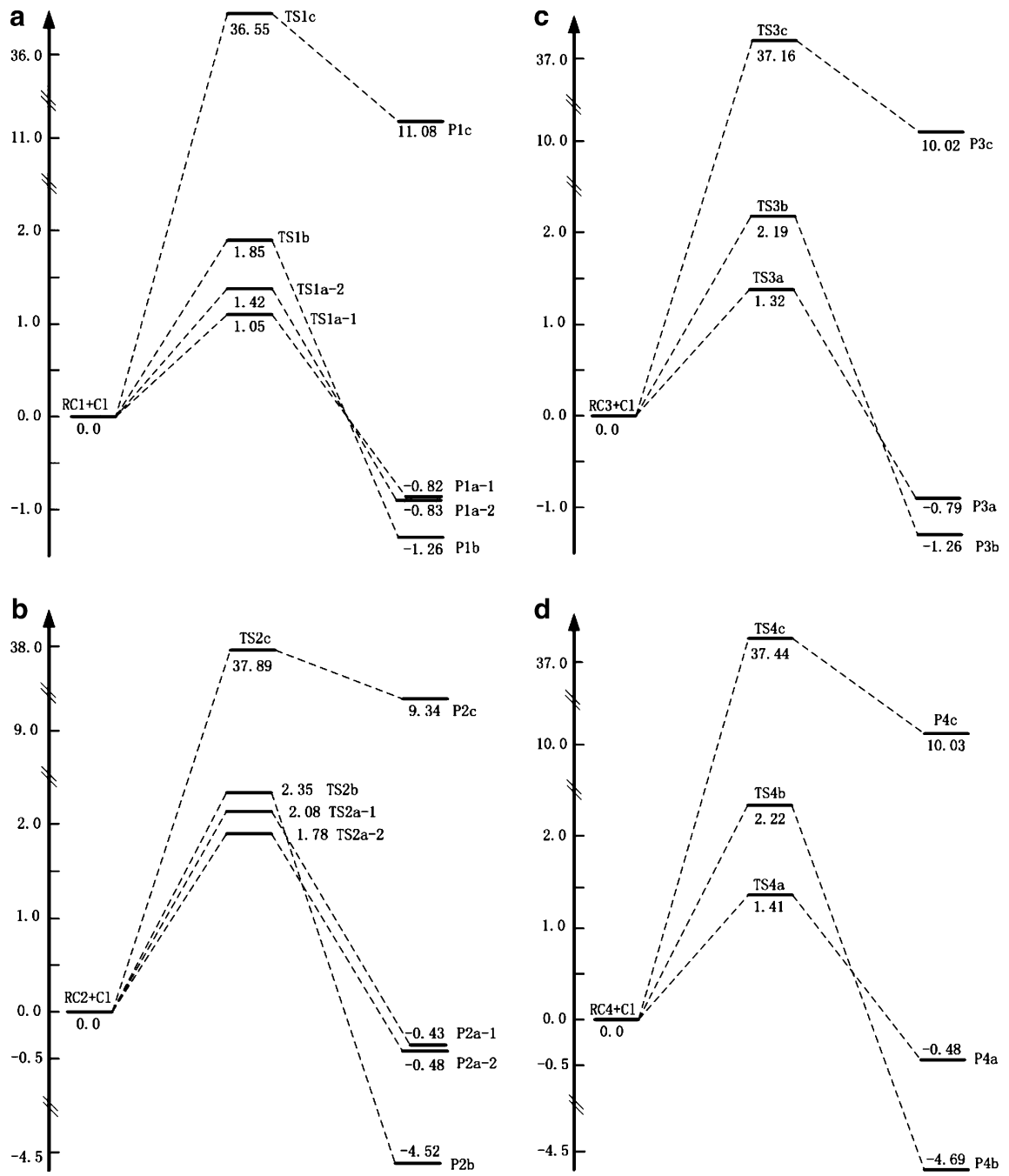


**Fig. 3** Schematic pathway for **a** RC1 + Cl → products, **b** RC2 + Cl → products, **c** RC3 + Cl → products, and **d** RC4 + Cl → products. Relative energies with ZPE correction at the BB1K/6-31 + G(d,p) level are in kcal/mol

**Table 2** The enthalpy of reaction at 298 K (kcal/mol) for each H-abstraction channel at the BB1K/6-31 + G(d,p) level

| | R1a-1 | R1a-2 | R1b | R2a-1 | R2a-2 | R2b | R3a | R3b | R4a | R4b |
|---|---|---|---|---|---|---|---|---|---|---|
| $\Delta H^{\circ}_{298}$ | −0.19 | −0.18 | −0.69 | 0.16 | 0.11 | −3.98 | −0.17 | −0.65 | −0.04 | −4.06 |

increases and becomes the major one at high temperatures. However, if we consider the two hydrogen atoms in the $-CH_3$ group are indistinguishable, that is, $k_{1a} = k_{1a\text{-}1} + k_{1a\text{-}2}$, we can conclude that the H-abstraction mainly occurs at the $-CH_3$ site, while the H-abstraction at the –CHO site becomes more and more important with the temperature increasing. Similar conclusion can be drawn for RC3. While the cases are slightly different for conformers RC2

**Table 3** Enthalpies of formation (kcal/mol) of $CH_3OCF_2CF_2OCHO$, $CH_2OCF_2CF_2OCHO$, and $CH_3OCF_2CF_2OCO$ at the BB1K/6-31 + G(d,p) level

| | $CH_3OCF_2CF_2OCHO$ | $CH_2OCF_2CF_2OCHO$ | $CH_3OCF_2CF_2OCO$ |
|---|---|---|---|
| R1 | −328.14 ± 0.12 | −279.95 ± 0.69[a] | −286.07 ± 0.71 |
| | | −279.93 ± 0.69[b] | |
| R2 | −327.68 ± 0.12 | −279.14 ± 0.69[c] | −288.90 ± 0.71 |
| | | −279.19 ± 0.69[d] | |
| R3 | −328.12 ± 0.12 | −279.91 ± 0.69 | −286.01 ± 0.71 |
| R4 | −327.35 ± 0.12 | −279.01 ± 0.69 | −288.66 ± 0.71 |

[a] For P1a-1; [b] For P1a-2; [c] For P2a-1; [d] For P2a-2

**Table 4** Rate constants ($k_n$, in $cm^3$ $molecule^{-1}$ $s^{-1}$) for the reactions R1-4 and the overall rate constant ($k_{overall}$) in the temperature range 200–2,000 K at the BB1K/6-31 + G(d,p) level

| $T$ | $k_1$ | $\omega_1$ | $k_2$ | $\omega_2$ | $k_3$ | $\omega_3$ | $k_4$ | $\omega_4$ | $k_{overall}$ |
|---|---|---|---|---|---|---|---|---|---|
| 200 | 8.36E−14 | 0.403 | 1.78E−14 | 0.144 | 5.64E−14 | 0.403 | 7.17E−14 | 0.050 | 6.26E−14 |
| 296 | 3.48E−13 | 0.365 | 1.13E−13 | 0.182 | 2.44E−13 | 0.365 | 3.60E−13 | 0.089 | 2.69E−13 |
| | | | | | | | | | (1.81 ± 0.36)E−13[a] |
| 298 | 3.57E−13 | 0.364 | 1.16E−13 | 0.182 | 2.50E−13 | 0.364 | 3.69E−13 | 0.090 | 2.75E−13 |
| 400 | 9.56E−13 | 0.339 | 3.72E−13 | 0.202 | 6.65E−13 | 0.339 | 1.06E−12 | 0.119 | 7.51E−13 |
| 500 | 1.95E−12 | 0.323 | 8.36E−13 | 0.214 | 1.34E−12 | 0.323 | 2.21E−12 | 0.140 | 1.55E−12 |
| 600 | 3.45E−12 | 0.312 | 1.56E−12 | 0.221 | 2.33E−12 | 0.312 | 3.95E−12 | 0.155 | 2.76E−12 |
| 800 | 8.24E−12 | 0.297 | 3.93E−12 | 0.230 | 5.38E−12 | 0.297 | 9.49E−12 | 0.176 | 6.62E−12 |
| 1,000 | 1.58E−11 | 0.288 | 7.73E−12 | 0.234 | 1.01E−11 | 0.288 | 1.82E−11 | 0.190 | 1.27E−11 |
| 1,200 | 2.65E−11 | 0.282 | 1.32E−11 | 0.237 | 1.65E−11 | 0.282 | 3.05E−11 | 0.199 | 2.13E−11 |
| 1,400 | 4.05E−11 | 0.277 | 2.04E−11 | 0.239 | 2.47E−11 | 0.277 | 4.65E−11 | 0.206 | 3.25E−11 |
| 1,700 | 6.78E−11 | 0.273 | 3.48E−11 | 0.241 | 4.04E−11 | 0.273 | 7.77E−11 | 0.213 | 5.45E−11 |
| 2,000 | 1.03E−10 | 0.269 | 5.33E−11 | 0.243 | 6.01E−11 | 0.269 | 1.18E−10 | 0.219 | 8.25E−11 |

[a] The experimental data from Reference [6]

and RC4. For those two reactions, the H-abstraction channel from the $-CH_3$ group is the predominant channel over the whole temperature range, and the H-abstraction from the –CHO group is the minor one, with the $k_{2b}/k_2$ value of RC2 ranging from 0.03 at 200 K to 0.08 at 2,000 K.

The overall rate constant ($k_{overall}$) for the reaction of $CH_3OCF_2CF_2OCHO + Cl \rightarrow$ products can be obtained from the following expression:

$$\begin{aligned} k_{overall} &= \omega_1 k_1 + \omega_2 k_2 + \omega_3 k_3 + \omega_4 k_4 \\ &= \omega_1(k_{1a-1} + k_{1a-2} + k_{1b}) + \omega_2(k_{2a-1} + k_{2a-2} + k_{2b}) \\ &\quad + \omega_3(k_{3a} + k_{3b}) + \omega_4(k_{4a} + k_{4b}) \\ &= k_{1T} + k_{2T} + k_{2T} + k_{4T} \end{aligned} \quad \text{(E1)}$$

where $\omega_i$ ($i = 1$–4) is the weight factor of conformer (RC1-4) and defined as

$$\omega_i = \frac{\exp(-\Delta E_i/RT)}{\sum_{i=1}^{4}\exp(-\Delta E_i/RT)} \quad \text{(E2)}$$

where $R$ is the gas constant and $\Delta E_i$ is the energy difference between RCi ($i = 1$–4) and RC1. The values of $\omega_i$ ($i = 1$–4) and overall rate constants are also listed in Table 4. From the weight factors of conformers ($\omega_i$, $i = 1$–4), it is very easy to find the degree of each conformer contributing to the overall rate constant. For example, the values of $\omega_1$, $\omega_2$, $\omega_3$, and $\omega_4$ are 0.403, 0.144, 0.403, and 0.05 at 200 K and 0.269, 0.243, 0.269, and 0.219 at 2,000 K, respectively. The theoretical rate constant of $2.69 \times 10^{-13}$ $cm^3$ $molecule^{-1}$ $s^{-1}$ at 296 K is in good agreement with the experimental value ($(1.81 \pm 0.36) \times 10^{-13}$ $cm^3$ $molecule^{-1}$ $s^{-1}$) determined by Wallington et al. [6]. The temperature dependence of the contribution of each conformer to the title reaction ($k_{nT}/k_{overall}$) is plotted in Fig. 5. It is seen that the $k_{1T}/k_{overall}$, $k_{2T}/k_{overall}$, $k_{3T}/k_{overall}$, and $k_{4T}/k_{overall}$ ratios are 0.54, 0.04, 0.36, and 0.06 at 200 K, respectively, which means RC1 is the most important conformer, which contributes to the title reaction, and RC3 is the secondary one, whereas RC2 and RC4 have negligible contribution at low temperatures. While as temperature increases, the ratios of $k_{1T}/k_{overall}$ and $k_{3T}/k_{overall}$ decrease whereas the ratios of $k_{2T}/k_{overall}$ and $k_{4T}/k_{overall}$ increase, especially at $T = 800$ K and above, $k_{4T}/k_{overall}$ increases dramatically. For example, the fractions are 0.36, 0.14, 0.23, and 0.27 for $k_{1T}/k_{overall}$, $k_{2T}/k_{overall}$, $k_{3T}/k_{overall}$, and $k_{3T}/k_{overall}$ at 1,000 K, respectively,

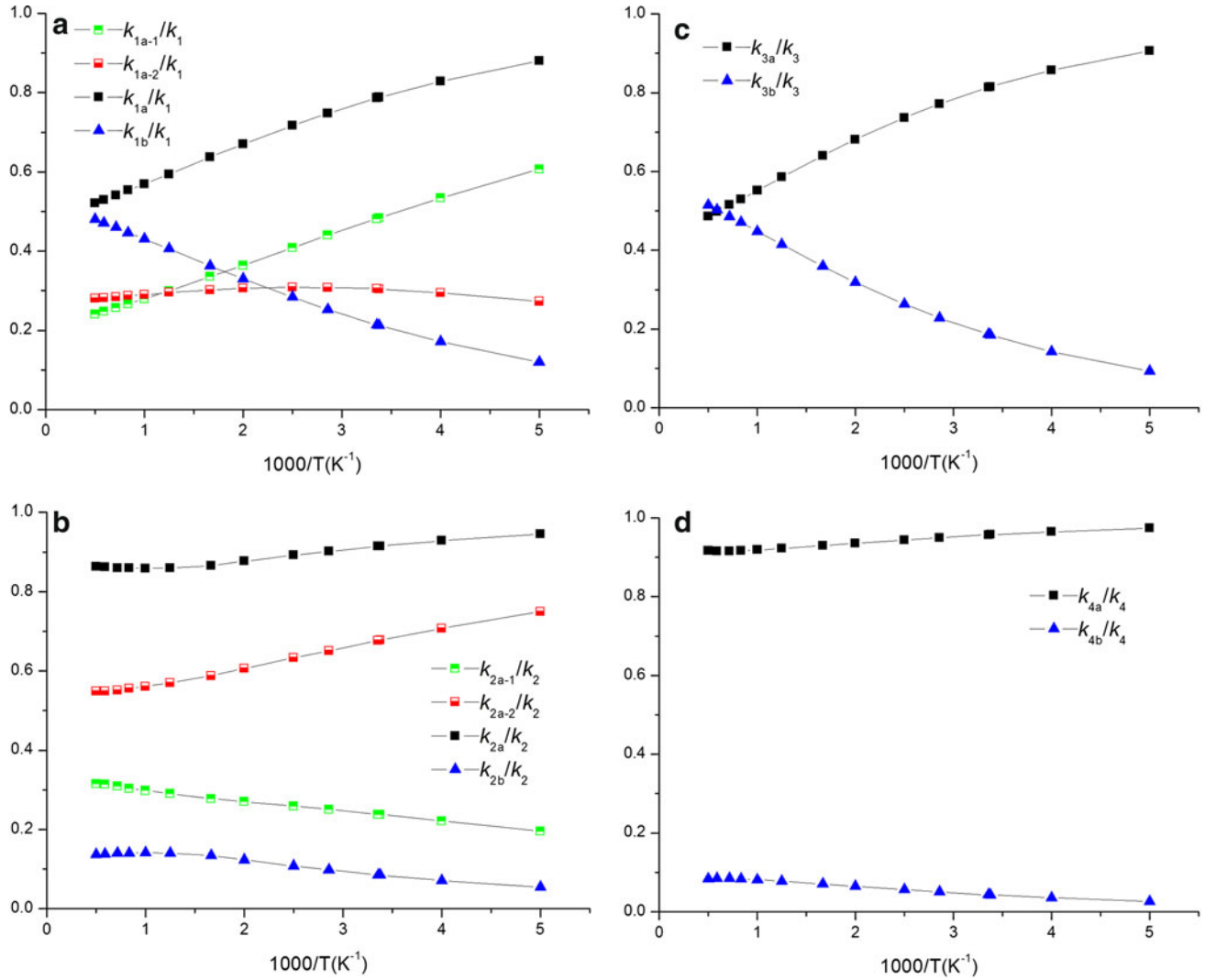


**Fig. 4** The calculated branching ratios vs 1,000/T between 200 and 2,000 K for **a** RC1 + Cl → products, **b** RC2 + Cl → products, **c** RC3 + Cl → products, and **d** RC4 + Cl → products

and the fractions of $k_{nT}/k_{overall}$ decrease in the order of $k_{1T}/k_{overall} > k_{4T}/k_{overall} > k_{3T}/k_{overall} > k_{2T}/k_{overall}$ when the temperature is higher than 800 K, indicating that H-abstraction reactions from RC1 and RC4 dominate the reaction at high temperatures.

Since there is a lack of experimental data at other temperatures except for 296 K, to facilitate future experimental study, the overall rate constants are fitted to a four-parameter rate-temperature formula, which was proposed by Truhlar et al. [29]. This four-parameter model is used here because it could provide a good representation of the temperature dependence over the whole temperature range of 200–2,000 K for the title reaction. The fitted expression is given as follows (in cm$^3$ molecule$^{-1}$ s$^{-1}$),

$$k_{overall} = 7.659 \times 10^{-18} T^{2.178} \times \exp\left[-768.9(T - 60.20)/\left(T^2 + 3623.44\right)\right] \quad \text{(E3)}$$

## 4 Summary and conclusions

In this paper, theoretical study for the reaction of $CH_3OCF_2CF_2OCHO$ + Cl has been carried out using the direct dynamics method. The PES information is obtained at the BB1K/6-31 + G(d,p) level, and the ICVT/SCT rate constants of each H-abstraction channel have been calculated over 200–2,000 K. The main results are as follows:

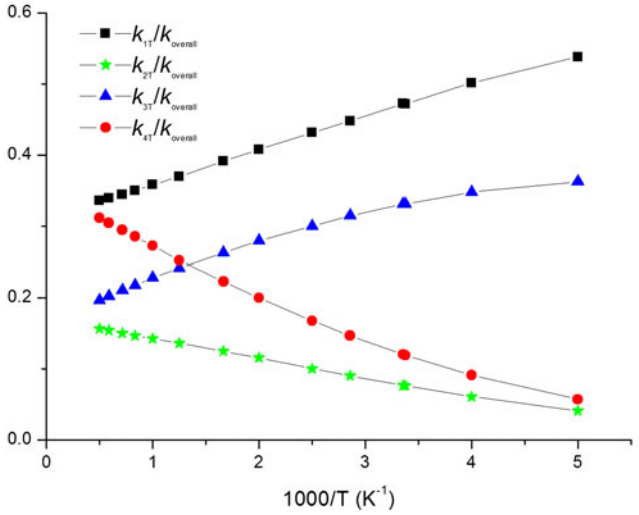


**Fig. 5** Plot of the calculated branching ratios ($k_n/k_{overall}$) versus 1,000/T between 200 and 2,000 K

1. The contributions of the four stable conformers of $CH_3OCF_2CF_2OCHO$ to the global rate constant have been considered due to the small energy differences between them. For each conformer, the H-abstraction channels from the $–CH_3$ and –CHO groups and the displacement channel attacked at the α-C were identified. The calculated energetic results show that the displacement channel can be negligible due to the high energy barrier and endothermicity. Also, the enthalpies of formation ($\Delta H_{f,298^\circ}$) for the reactants and the product radicals, which are lack of experimental data, were estimated via isodesmic reactions.
2. The kinetic calculations show that for RC1 and RC3, the H-abstraction reactions mainly take place at the $–CH_3$ site, especially at the low temperatures, while the H-abstraction from the –CHO group becomes a competitive channel with the temperature increasing; for RC2 and RC4, the H-abstraction channel from the $–CH_3$ group is the predominant one over the whole temperature range.
3. The overall rate constant of the title reaction was obtained by considering the weight factors of the four conformers calculated from the Boltzmann distribution function. The theoretical value of $k_{overall}$ at 296 K is $2.69 \times 10^{-13}$ cm$^3$ molecule$^{-1}$ s$^{-1}$, in good agreement with the available experimental data. To provide good estimation for further experimental study, the fitted four-parameter rate constant expression for the title reaction within 200–2,000 K is given as: $k_{overall} = 7.659 \times 10^{-18} T^{2.178} \exp[-768.9(T - 60.20)/(T^2 + 3623.44)]$.
4. The calculated results show that RC1 is the most important conformer to the title reaction and RC3 is the secondary one at low temperature range, while as temperature increases, RC4 becomes more important and the fractions of $k_{nT}/k_{overall}$ decrease in the order of $k_{1T}/k_{overall} > k_{4T}/k_{overall} > k_{3T}/k_{overall} > k_{2T}/k_{overall}$ at 800 K and above, thus RC1 and RC4 have the dominant contribution to the title reaction at high temperatures.

**Acknowledgments** We thank Professor Donald G. Truhlar for providing the POLYRATE 9.7 program. This work is supported by the National Nature Science Foundation of China (20973077, 20303007) and the Program for New Century Excellent Talents in University (NCET).

## References

1. Marchionni G, Visca M, Eur Pat Appl. 1275678A 2003 (Chem Abs 138, 90675)
2. Sianesi D, Marchionni G, De Pasquale RJ (1994) In: Banks RE (ed) Organofluorine chemistry: principles and commercial applications. Plenum Press, New York
3. Marchionni G, Ajroldi G, Pezzin G (1996) In: Agarwal SL, Russom S (eds) Comprehensive polymer science (Second Supplement). Pergamon, London
4. Marchionni G, Guarda PA (1998) U.S. Patent, 5,744,651
5. Yu HB, Cui FC, Wang YX, Liu HX, Liu JY (2011) J Theor Comp Chem 10:231–244
6. Sulback Andersen MP, Hurley MD, Wallington TJ, Blandini F, Jensen NR, Librando V, Hjorth J, Marchionni G, Avataneo M, Visca M, Nicolaisen FM, Nielsen OJ (2004) J Phys Chem A 108:1964–1972
7. Zhao Y, Lynch BJ, Truhlar DG (2004) J Phys Chem A 108:2715
8. Truhlar DG, Garrett BC (1980) Acc Chem Res 13:440
9. Truhlar DG, Isaacson AD, Garrett BC (1985) Generalized transition state theory. In: Baer M (ed) The theory of chemical reaction dynamics, vol 4. CRC Press, Boca Raton, p 65
10. Truhlar DG, Garrett BC (1984) Annu Rev Phys Chem 35:159
11. Frisch MJ, Trucks GW, Schlegel HB, Scuseria GE, Robb MA, Cheeseman JR, ScalmaniG, Barone V, Mennucci B, Petersson GA, Nakatsuji H, Caricato M, Li X, Hratchian HP, Izmaylov AF, Bloino J, Zheng G, Sonnenberg JL, Hada M, Ehara M, Toyota K, Fukuda R, Hasegawa J, Ishida M, Nakajima T, Honda Y, Kitao O, Nakai H, Vreven T, Montgomery JA Jr, Peralta JE, Ogliaro F, Bearpark M, Heyd JJ, Brothers E, Kudin KN, Staroverov VN, Kobayashi R, Normand J, Raghavachari K, Rendell A, Burant JC, Iyengar SS, Tomasi J, Cossi M, Rega N, Millam NJ, Klene M, Knox JE, Cross JB, Bakken V, Adamo C, Jaramillo J, Gomperts R, Stratmann RE, Yazyev O, Austin AJ, Cammi R, Pomelli C, Ochterski JW, Martin RL, Morokuma K, Zakrzewski VG, Voth GA, Salvador P, Dannenberg JJ, Dapprich S, Daniels AD, Farkas O, Foresman JB, Ortiz JV, Cioslowski J, Fox DJ (2009) Gaussian 09, revision A.1. Gaussian, Inc., Wallingford, CT
12. Becke AD (1988) Phys Rev A 38:3098
13. Becke AD (1996) J Chem Phys 104:1040
14. Zhao Y, Gonzales-Garcia N, Truhlar DG (2005) J Phys Chem A 109:2012
15. Parveen S, Chandra AK (2009) J Phys Chem A 113:177–183
16. Gao H, Wang YX, Liu JY, Yang L, Li ZS, Sun CC (2008) J Phys Chem A 112:4176–4185
17. Hemelsoet K, Moran D, Speybroeck VV, Waroquier M, Radom L (2006) J Phys Chem A 110:8942
18. Corchado JC, Chuang YY, Fast PL, Hu WP, Liu YP, Lynch GC, Nguyen KA, Jackels CF, Ramos AF, Ellingson BA, Lynch BJ,

Melissas VS, Villa J, Rossi I, Coitino EL, Pu J, Albu TV, Steckler R, Garrett BC, Isaacson AD, Truhlar DG (2007) POLYRATE, version 9.7. University of Minnesota, Minneapolis
19. Garrett BC, Truhlar DG, Grev RS, Magnuson AW (1980) J Phys Chem 84:1730–1748
20. Lu DH, Truong TN, Melissas VS, Lynch GC, Liu YP, Grarrett BC, Steckler R, Issacson AD, Rai SN, Hancock GC, Lauderdale JG, Joseph T, Truhlar DG (1992) Comput Phys Commun 71:235
21. Liu Y-P, Lynch GC, Truong TN, Lu D-H, Truhlar DG, Garrett BC (1993) J Am Chem Soc 115:2408
22. Piter KS, Gwinn WD (1942) J Chem Phys 10:428
23. Piter KS (1946) J Chem Phys 14:239
24. Truhlar DG (1991) J Comput Chem 12:266–270
25. Chuang YY, Truhlar DG (2000) J Chem Phys 112:1221
26. Chuang YY, Truhlar DG (2004) J Chem Phys 121:7036
27. Chuang YY, Truhlar DG (2006) J Chem Phys 124:179903
28. Ellingson BA, Lynch VA, Mielke SL, Truhlar DG (2006) J Chem Phys 125:084305
29. Zheng JJ, Truhlar DG (2010) Phys Chem Chem Phys 12:7782–7793
30. Linstrom PJ, Mallard WG (eds) (2009) Chemistry Webbook NIST. Available from: http://webbook.Nist.Gov/chemistry